

***In vivo* Actions of Insulin-like Growth Factor-I (IGF-I) on Brain Myelination: Studies of IGF-I and IGF Binding Protein-1 (IGFBP-1) Transgenic Mice**

Ping Ye, Johnny Carson, and A. Joseph D'Ercole

Department of Pediatrics, The University of North Carolina at Chapel Hill, Chapel Hill, North Carolina 27599-7220

To study the effects and mechanisms of insulin-like growth factor I (IGF-I) on brain myelination *in vivo*, the morphology of myelinated axons and the expression of myelin specific protein genes have been examined in transgenic (Tg) mice that overexpress IGF-I and that those ectopically express IGF binding protein-1 (IGFBP-1), a protein that inhibits IGF-I actions when present in molar excess. Our data show that the percentage of myelinated axons and the thickness of myelin sheaths are significantly increased in IGF-I Tg and decreased in the IGFBP-1 mice. Cerebral cortical proteolipid protein (PLP) and myelin basic protein (MBP) mRNAs consistently exhibit ~200% increases in IGF-I Tg mice and ~50% decreases in IGFBP-1 Tg mice. The percentage of oligodendrocytes labeled with a PLP cRNA probe in the corpus callosum and cerebral cortex also is increased in IGF-I Tg mice and reduced in IGFBP-1 Tg mice, suggesting that IGF-I promotes oligodendrocyte survival and/or proliferation. The alterations in the number of oligodendrocytes, however, can not completely account for the changes in myelin gene expression. These results strongly indicate that IGF-I increases myelination by increasing the number of myelinated axons and the thickness of myelin sheaths, the latter by mechanisms that involve stimulation of the expression of myelin protein genes and increase of oligodendrocyte number.

[Key words: oligodendrocyte, myelination, proteolipid protein (PLP), myelin basic protein (MBP), gene expression, IGF-I, IGFBP-1, transgenic mice]

The proliferation and differentiation of oligodendrocytes, and the myelination that ensues, are controlled by a number of soluble growth factors and neuronal influences (Chen and De Vries, 1989; Raff, 1989; Hunter and Bottenstein, 1991; Barres and Raff, 1993). Recent evidence suggests that insulin-like growth factor-I (IGF-I) has an important role in these processes. IGF-I stimulates proliferation and differentiation of oligodendrocyte progenitors in culture (McMorris et al., 1986; McMorris and Dubois-Dalcq, 1988; Mozell and McMorris, 1991) and promotes the survival of cultured oligodendrocytes (Barres et al., 1992). Dis-

ruption of the IGF-I gene significantly decreases oligodendrocyte number in mice (Beck et al., 1995). Both IGF-I (McMorris, personal communication) and the type I IGF receptor (McMorris et al., 1986; Baron-Van Evercooren et al., 1991; Masters et al., 1991) are expressed by oligodendrocytes and their progenitor cells and by neurons that are located nearby (Bartlett et al., 1991; Garcia-Segura et al., 1991). Furthermore, maximal IGF-I expression precedes the peak time of myelin-specific protein gene expression and rapid myelination (Sorg et al., 1987; Campagnoni, 1988; Rotwein et al., 1988; Bach et al., 1991; Bartlett et al., 1991).

The brains of transgenic (Tg) mice that overexpress human IGF-I (hIGF-I) exhibit a marked increase in myelin content (Carson et al., 1993). To explore the mechanisms of IGF-I's *in vivo* effects on oligodendrocyte development and on myelination, we have examined the morphology of myelinated axons and the expression of the genes for proteolipid protein (PLP) and myelin basic protein (MBP), the two most abundant myelin-specific proteins, utilizing two Tg mouse models of IGF actions. To evaluate the effects of IGF-I overexpression in brain, new lines of Tg mice were generated using the same hIGF-I fusion gene previously described in studies of IGF-I overexpressing Tg mice (Mathews et al., 1988; Behringer et al., 1990; Carson et al., 1993). To evaluate a decrease of IGF-I function in brain, we employed Tg mice that express human IGF binding protein-1 (hIGFBP-1) ectopically in brain (D'Ercole et al., 1994). The hIGFBP-1 expressed by these mice (IGFBP-1 Tg mice) is one of the family of IGF binding proteins that modulate the actions of the IGFs (IGF-I and IGF-II) by controlling their serum and tissue concentrations and bioavailability, as well as transporting IGFs from their sites of synthesis (see reviews: Lee et al., 1993; Jones and Clemmons, 1995). Depending upon its molar concentration, IGFBP-1 can inhibit the actions of the IGFs. In our studies of IGFBP-1 Tg mice (D'Ercole et al., 1994), we have observed brain growth retardation. As judged by total DNA content, cell number is decreased in these mice. The reduction, however, is not as great as the reduction in brain weight, suggesting that other components of the brain, such as myelin, also are involved.

Using these alternative models of IGF-I overexpression and of decreased IGF bioavailability, we report evidence that IGF-I increases myelination by increasing both the number of myelinated axons and the thickness of myelin sheaths, the latter by mechanisms that involve stimulation of myelin-specific protein gene expression and promotion of oligodendrocyte proliferation and/or survival.

Materials and Methods

Animals. IGF-I Tg mice were generated by classical microinjection methodology using the same mouse metallothionein-I (MT-I) pro-

Received Apr. 27, 1995; revised July 3, 1995; accepted July 6, 1995.

We thank Dr. Gabriel Gutierrez-Ospina for helpful discussion, and Ms Yuzhi Xing and Mrs. Nancy Hu for their technical assistance. P.Y. was supported by NIH Training Grant T32DK07129. This work was supported by Grant HD08299 to A.J.D. from NICHD.

Correspondence should be addressed to Dr. A. J. D'Ercole, Department of Pediatrics, CB# 7220, University of North Carolina at Chapel Hill, Chapel Hill, NC 27599-7220.

Copyright © 1995 Society for Neuroscience 0270-6474/95/157344-13\$05.00/0

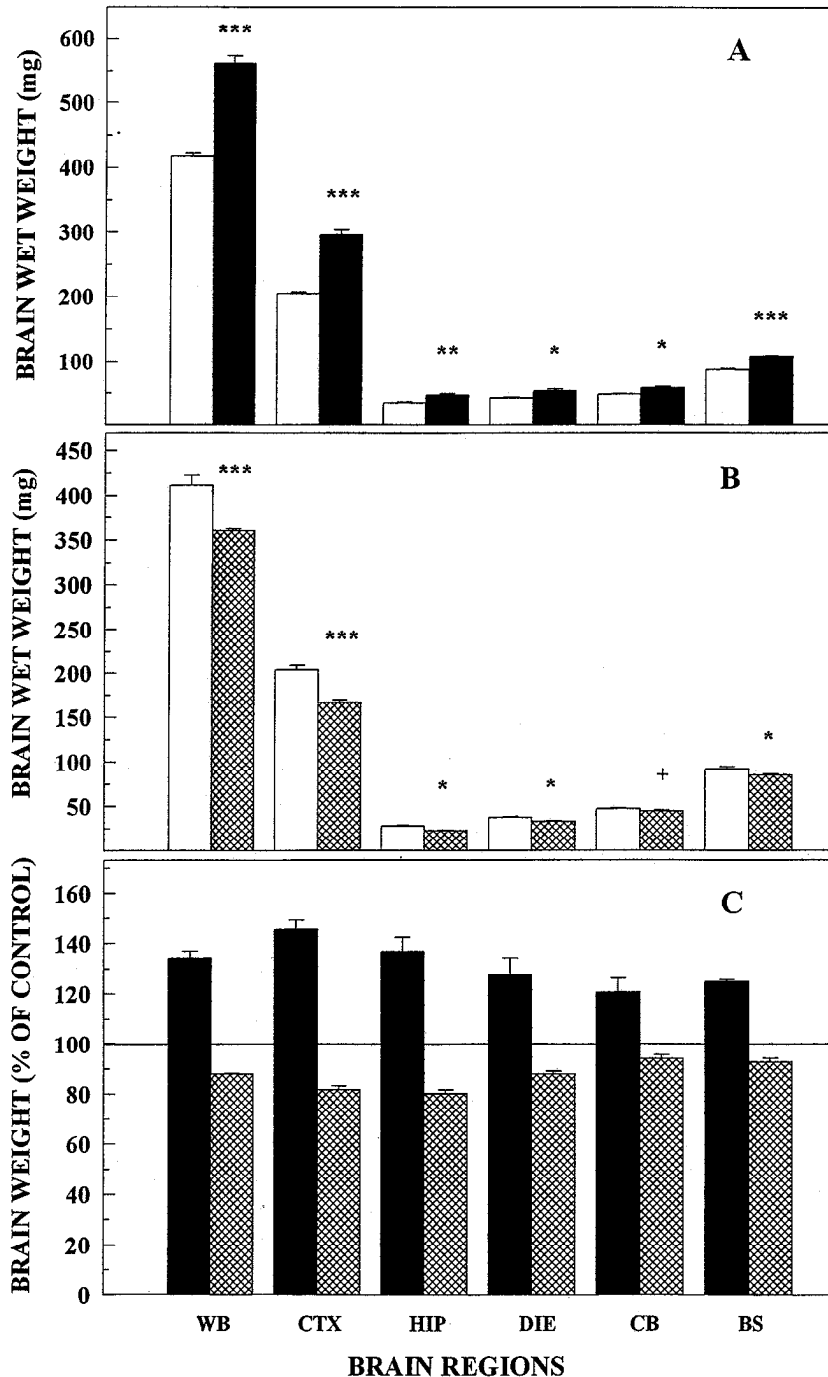


Figure 1. Whole brain and regional weight in IGF-I (A) and IGFBP-1 (B) Tg mice. Brains were collected and dissected from 35 d old IGF-I Tg mice (solid bars), IGFBP-1 Tg mice (hatched bars) and their littermate controls (open bars). Values are means \pm SE from four to six mice. C depicts brain weight data shown in A and B presented as percentage of littermate controls. WB, Whole brain; CTX, cerebral cortex; HIP, hippocampus; DIE, diencephalon; CB, cerebellum; and BS, brainstem. Statistical comparisons with normal littermates were made using Student's *t* test. +, $P < 0.1$; *, $P < 0.05$; **, $P < 0.01$; ***, $P < 0.001$.

moter-driven hIGF-I fusion gene as previously reported to create the original line of these mice (Mathews et al., 1988) in the Transgenic Core Facility at the University of North Carolina at Chapel Hill. A single line (line 52) of these IGF-I Tg mice was used in this study because its transgene is relatively better expressed in brain than in other organs, as judged by the mRNA and protein levels, and immunostaining intensity (D'Ercole and Ye, unpublished data). As a result, the brains of these Tg mice are overgrown (see Results). However, there is no elevation in serum IGF-I concentrations, nor is there an increase in the body weights in these Tg mice. IGFBP-1 Tg mice, also driven by MT-I promoter, have been described in detail in our previous reports (Dai et al., 1994; D'Ercole et al., 1994). These mice express IGFBP-1 ectopically in brain, which results in retardation of brain growth that is apparent by the second week of postnatal life. In this study, we have used the B line exclusively.

Both IGF-I and IGFBP-1 Tg mice were bred as heterozygotes in

order to obtain non-transgenic littermate mice to serve as normal controls. To generate mice carrying both IGF-I and IGFBP-1 transgenes (IGF-I/IGFBP-1 mice), male heterozygous IGF-I Tg mice were bred with female heterozygous IGFBP-1 Tg mice. This mating yielded mice with about 25% of each the following genotypes: nontransgenic normal mice, IGF-I Tg mice, IGFBP-1 Tg mice, and the mice carrying both IGF-I and IGFBP-1 transgenes (IGF-I/IGFBP-1). All mice were fed standard laboratory chow. To insure maximum expression of the transgenes, mice were provided drinking water supplemented with 10 mM ZnSO₄ from 2–3 d after birth and 25 mM ZnSO₄ from about 25 d of age (Dai et al., 1994). Their environment was maintained with 12:12 hr (light:dark) cycles at 22°C.

The genotypes of mice initially were determined by polymerase chain reaction (PCR) of mouse tail genomic DNA, and further confirmed by Northern or Southern blot analysis for the transgene. All procedures

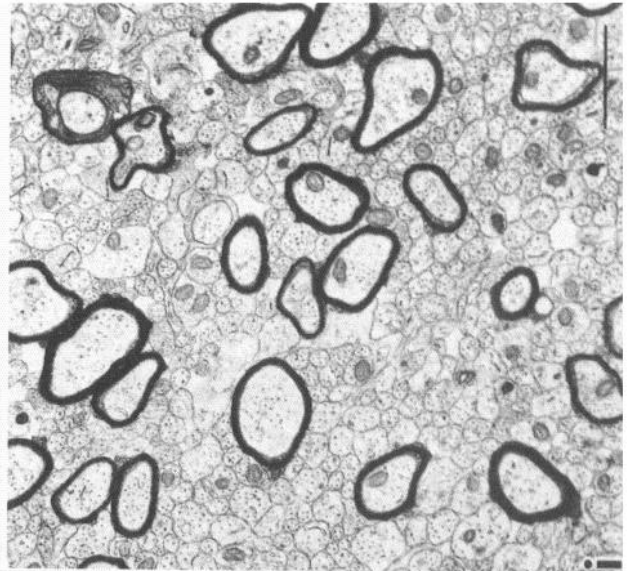
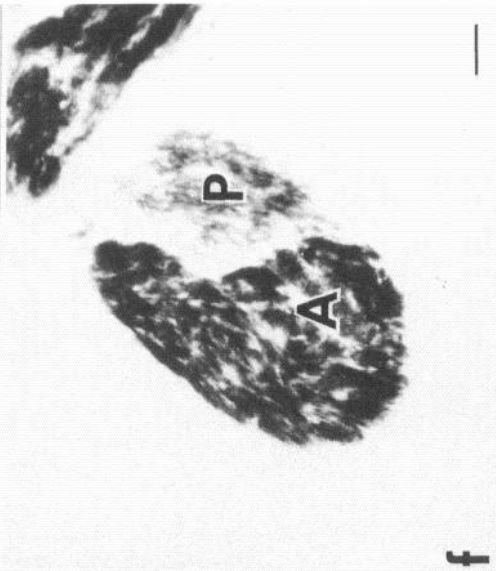
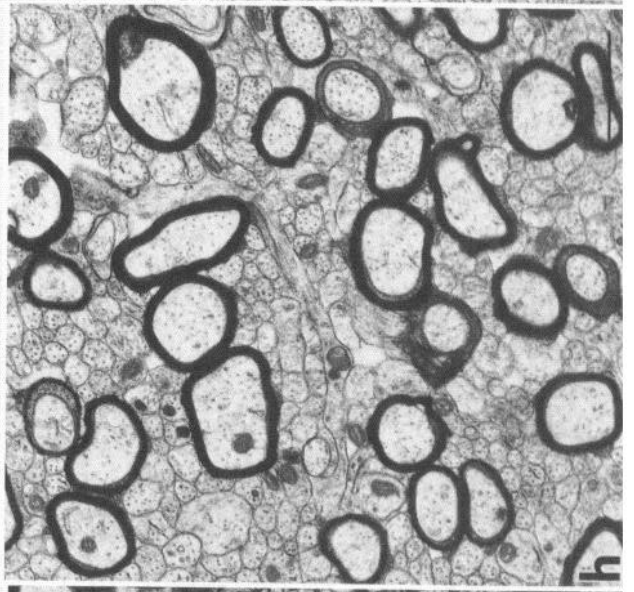
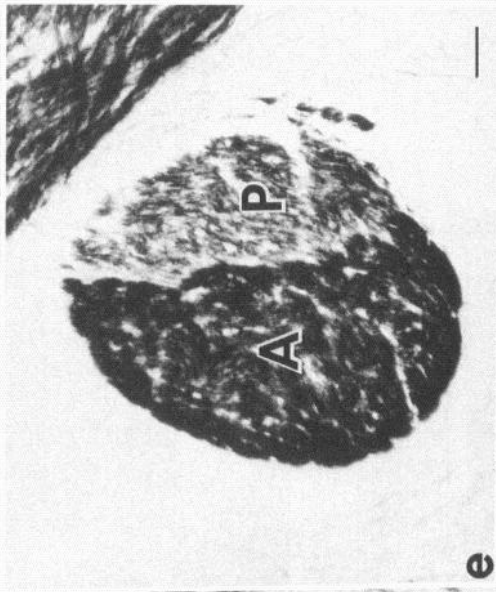
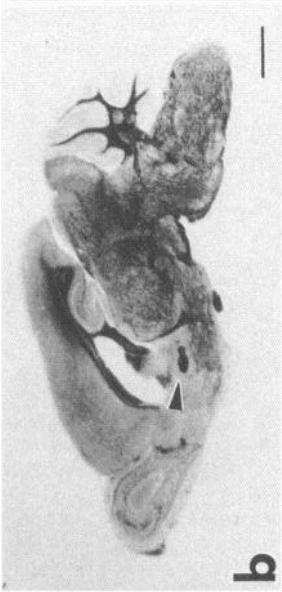
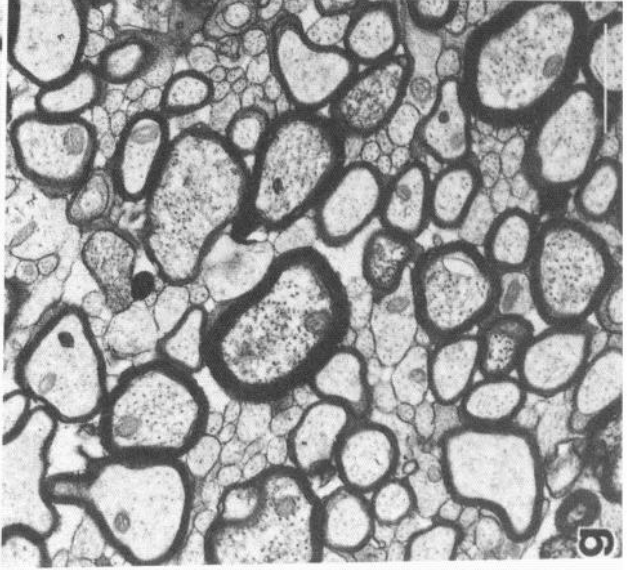
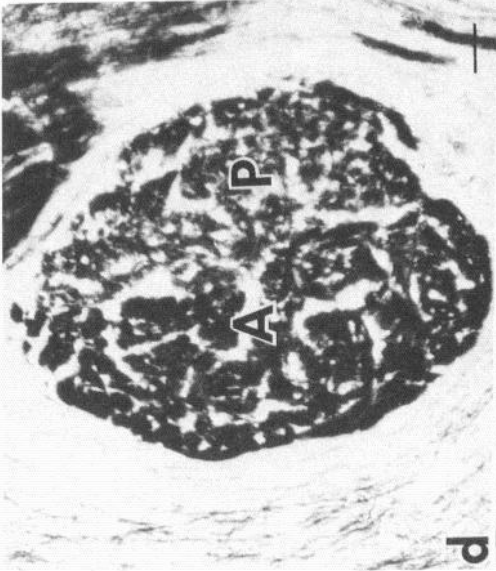


Table 1. The percentage of myelinated axons in IGF-I Tg and IGFBP-1 Tg mice

	Percentage of myelinated axons in anterior commissure (means \pm SE)			
	Anterior part		Posterior part	
	35 d	68 d	35 d	68 d
Littermate control	29.71 \pm 1.64	39.84 \pm 0.57	12.90 \pm 0.72	18.41 \pm 1.37
IGF-I Tg	32.40 \pm 0.87!!	39.04 \pm 0.85!	14.50 \pm 1.93!	24.81 \pm 0.51*!!!
IGFBP-1	22.62 \pm 1.22*	36.30 \pm 0.41*	7.07 \pm 0.60**	13.63 \pm 0.50*

Three each of IGF-I Tg, IGFBP-1 Tg, and normal control mice were transcardially perfused with glutaraldehyde and paraformaldehyde. Electron microphotographs of AC were taken, and the number of myelinated axons was counted on each photograph. Values are means \pm SE. *, $p < 0.05$; **, $p < 0.01$ versus control mice. !, $p < 0.05$; !!, $p < 0.01$; and !!!, $p < 0.001$ versus IGFBP-1 mice.

used were approved by institutional review committee of the University of North Carolina at Chapel Hill.

Probes. PLP and MBP cDNAs were generated from mouse brain total RNA by reverse transcription-PCR (RT-PCR) using specific antisense 20-mer oligonucleotide primers and Moloney murine leukemia virus reverse transcriptase (United States Biochemical, Cleveland, OH) according to the manufacturer's protocol. Cyclophilin cDNA was produced from rat liver total RNA by RT-PCR. The fragments which corresponded to base pairs (bp) 268–903 of the mouse PLP cDNA (Hudson et al., 1987), 58–490 of the mouse MBP cDNA (Newman et al., 1987), and 106–517 of the rat cyclophilin cDNA (Danielson et al., 1988) were amplified by PCR (GeneAmp DNA Amplification Reagent Kit, Perkin-Elmer/Cetus, Norwalk, CT), also using 20-mer oligonucleotide primers. The DNA fragments were subsequently cloned into the cloning site of pCR-II vector (Invitrogen, San Diego, CA). The identity of these DNA fragments was confirmed by the dideoxy sequencing method using T7 sequenase (United States Biochemical, Cleveland, OH). Human IGF-I and IGFBP-1 DNA fragments, respectively, were amplified from the plasmids containing the transgenes (Mathews et al., 1988; Dai et al., 1994). The amplified fragments corresponded to base pairs 179–537 of the IGF-I cDNA (Jansen et al., 1983) and 437–660 IGFBP-1 cDNA (Brewer et al., 1988), respectively. Single stranded DNA (ssDNA) hybridization probes were generated from these templates by linear PCR (Konat et al., 1991; Ye et al., 1992) using their respective 3' end primers and 32 P-labeled dCTP (Amersham, Arlington Heights, IL).

Northern blot analysis. Mice were sacrificed by deep ether anesthesia, and brains were quickly removed and dissected. After dissection tissues

were homogenized within 4 M guanidinium thiocyanate. Total RNA was extracted using the acidic guanidinium thiocyanate-phenol-chloroform (AGPC) method (Chomczynski and Sacchi, 1987) and quantified spectrophotometrically at 260 nm. An aliquot of 6 or 10 μ g total RNA was electrophoresed on 1% denaturing agarose gel, transferred onto a GeneScreen membrane (Du Pont NEN, Boston, MA) and UV cross-linked followed by vacuum baking at 80°C for 2 hr. The filters were stained with 0.02% methylene blue and photographed to quantitate the amount of RNA transferred. The membrane was hybridized with radio-labeled ssDNA probes (see above) in Church's buffer (0.5 M sodium phosphate, pH 7.1/7% SDS/0.1 mM EDTA), and washed at high stringency (40 mM sodium phosphate with 0.2% SDS at 55–60°C for 60 min). The position of the specific messages was detected by autoradiography. After autoradiography, membranes were stripped in 20 mM sodium phosphate with 0.5 mM EDTA at 80–85°C for 30–60 min.

Quantification was performed using a computer-assisted image analysis system (Image-Pro, Media Cybernetics, Silver Spring, MD). The message levels were normalized to the cyclophilin mRNA abundance (Danielson et al., 1988; Jakubowski et al., 1991) or to the amount of total (ribosomal) RNA on the membrane to insure the accuracy of the changes in the myelin protein mRNA abundance and equal loading of RNA. In agreement with the previous report (Jakubowski et al., 1991), the cyclophilin mRNA levels were slightly decreased over the time period examined (7–42 d of age; Ye and D'Ercole unpublished data), however, there was no significant difference in cyclophilin mRNA abundance among IGF-I Tg and IGFBP-1 Tg mice and their normal littermates at any time studied. The abundance of the cyclophilin mRNA

Table 2. The thickness of myelin sheaths surrounding axons of different diameters in IGF-I and IGFBP-1 Tg mice

	Axon diameter (nm)	Thickness of myelin sheaths in axons of different diameter (nm, means \pm SE)		
		Control	MT-1/IGF-I	MT-1/IGFBP-1
Anterior part	300–399	68.49 \pm 1.12 (15.0)	79.43 \pm 1.72 (10.8)***!!!	70.31 \pm 1.47 (16.8)
	500–599	79.09 \pm 1.14 (24.5)	87.56 \pm 1.61 (23.1)***!!!	77.17 \pm 1.04 (23.4)^\wedge
	700–799	91.47 \pm 2.73 (7.4)	103.19 \pm 2.80 (10.1)**!!!	81.84 \pm 2.19 (8.3)**
Posterior part	300–399	64.10 \pm 1.38 (19.8)	67.91 \pm 1.32 (16.7)*!!!	59.48 \pm 1.55 (15.2)*
	500–599	70.00 \pm 1.48 (21.3)	76.41 \pm 1.48 (19.7)**!!!	67.36 \pm 1.23 (23.2)^\wedge^\wedge
	700–799	79.27 \pm 3.84 (5.6)	91.04 \pm 4.20 (9.4)+!	78.26 \pm 4.20 (6.2)

The AC from three IGF-I Tg and IGFBP-1 Tg mice and normal controls were electron microphotographed. The measurement of myelin sheath thickness and axon diameter on these photographs was made with assistant of Image-Pro system. The thickness of myelin sheaths on axons with similar diameter was analyzed. Values are means \pm SE. Relative number of axons analyzed (percentage of total myelinated axons) is given in parentheses. ^, $p < 0.2$; ^/^, $p < 0.1$; +, $p = 0.064$; *, $p < 0.05$; **, $p < 0.01$; and ***, $p < 0.001$ versus controls. !, $p < 0.05$; !!, $p < 0.01$; and !!!, $p < 0.001$ versus IGFBP-1 Tg mice.

Figure 2. Myelin staining of brain (a–c) and anterior commissure (d–f) and electron micrographs of posterior AC (g–i) in IGF-I Tg and IGFBP-1 Tg mice. For myelin staining, brains from 35 d old IGF-I (a, d) and IGFBP-1 (c, f) Tg mice, and a littermate control (b, e) were perfused and fixed with 4% paraformaldehyde, sagittally frozen-sectioned, and stained with 0.2% gold chloride. Arrowheads in a–c indicate anterior commissure. In high power micrographs of AC (d–f) the anterior part and posterior part are labeled with A and P, respectively. For electron microscopy, 68 d old mice were perfused with 2% glutaraldehyde and 2% paraformaldehyde. Micrographs of posterior AC were taken from IGF-I Tg mice (g), IGFBP-1 Tg mice (i), and control mice (h). Scale bars: a–c, 2 μ m; c–e, 50 μ m; g–i, 1.1 μ m.

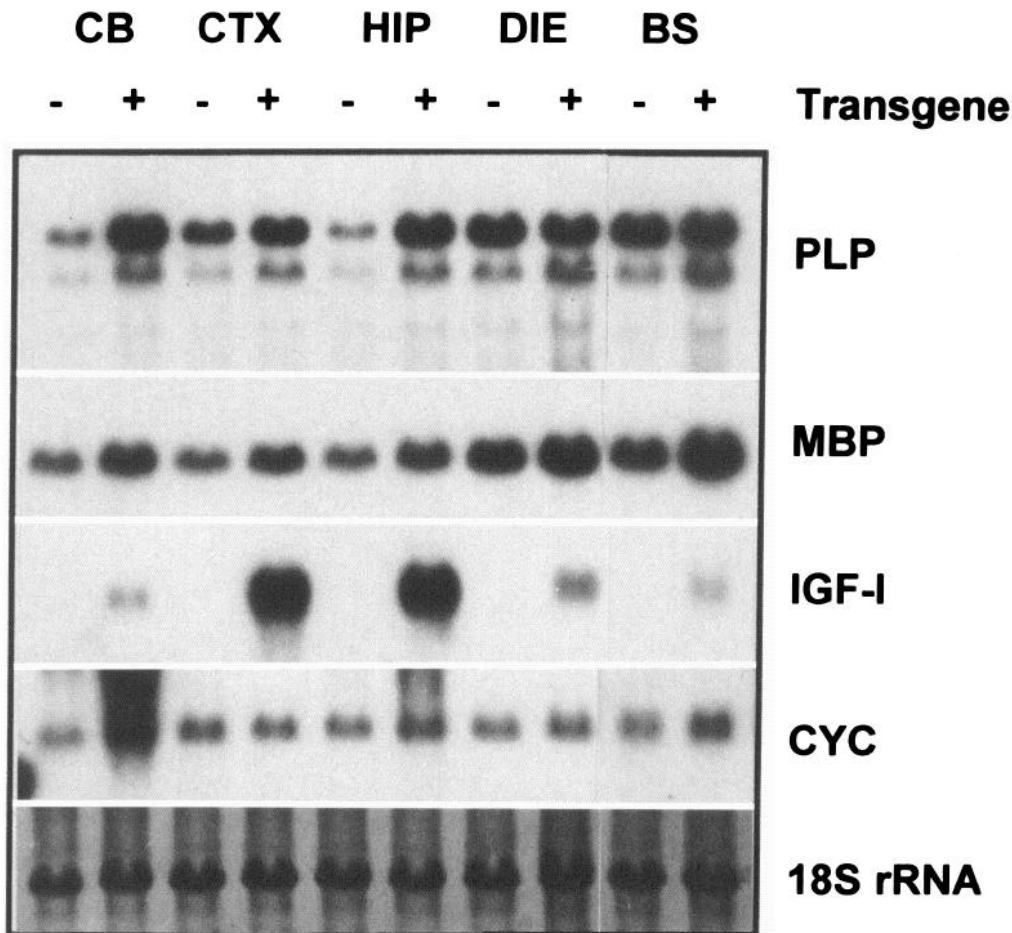


Figure 3. Expression of PLP and MBP genes in cerebral cortex (CTX), hippocampus (HIP), diacencephalon (DIE), brainstem (BS), and cerebellum (CB) of 35 d old IGF-I Tg mice. Ten micrograms of total RNA from tissues of IGF-I Tg mice and their littermate controls were applied to each lane. IGF-I Tg mice are indicated as (+) at the top of the figure, and littermate controls as (-). After hybridized with the PLP probe and autoradiography, the filters were stripped and reprobbed with MBP, IGF-I and cyclophilin (CYC) probes. The 18S rRNA panel shows methylene blue staining of the 18S rRNA band on blot.

also closely paralleled the amount of total RNA (18S and 28S rRNA) transferred as estimated by methylene blue staining.

Histological and histochemical analysis. For myelin staining, 35 d old IGF-I Tg, IGFBP-1 Tg mice, and their littermates ($n = 3$ for each) were transcardially perfused with 4% paraformaldehyde in phosphate-buffered saline (PBS), pH 7.4. Brains were removed and post-fixed in the same fixative containing 20% sucrose overnight at 4°C. Sagittal sections (25 μ m) were cut on a cryostat, mounted onto gelatin-coated slides and stored at -80°C until use. Myelinated fibers were stained using the gold chloride method as described by Schmued (1990). Briefly, the sections were washed with distilled water and incubated with 0.2% gold chloride (Sigma Chemical, St. Louis, MO) in 0.02 M neutral phosphate buffer with 0.9% NaCl for 2–4 hr at room temperature (RT) or at 42°C. After a brief wash with distilled water, sections were fixed with 2.5% sodium thiosulfate and mounted.

For electron microscopic examination, groups of 3 IGF-I Tg, IGFBP-1 Tg mice and normal littermates at 35 or 68 d of age were perfused and fixed with 2% glutaraldehyde and 2% paraformaldehyde in PBS. The brains were sagittally sliced in ~0.5 mm of thickness. The region containing the anterior commissure was blocked out and directionally embedded in epon. Semithin sections (~1 μ m) were performed to ensure the location of the anterior commissure. Because of large difference in the morphology and the number of myelinated axons between anterior and posterior parts of mouse anterior commissure, six to nine photographs were randomly taken from each anterior and posterior part of anterior commissure at 7000 \times , respectively. The number of myelinated axons and the thickness of myelin sheaths were measured on these photographs with the aid of the Image-Pro analysis system. There were no abnormalities in myelin and axon structure observed in

either IGF-I or IGFBP-1 Tg mice. The measurement of the thickness of myelin sheaths was taken from the straight and circular fibers, in which both the inner and outer surface of the myelin sheath stood out as sharp, equidistant and parallel lines. The diameter of axons was calculated from the circumference of the inner surface of the myelin sheaths on these fibers. Six to nine thousand axons from the anterior and posterior part of the anterior commissure in each group of mice were counted. Over 1000 and 500 myelinated axons were measured for the thickness of myelin sheaths in the anterior and posterior part of anterior commissure, respectively.

In situ hybridization was performed as described (Zimmermann et al., 1993; Stenvers et al., 1994) except that a digoxigenin-labeled PLP cRNA probe (Dig-riboprobe) and colorimetric detection were employed. After fixation with 4% paraformaldehyde in (PBS), the frozen-cut sections (10 μ m) were treated with 0.2 N HCl, extensively washed with PBS and hybridized with antisense PLP Dig-riboprobe generated from the mouse PLP cDNA-containing plasmid (see above Probes section) using Genius RNA Labeling kit (Boehringer Mannheim, Indianapolis, IN) and T7 RNA polymerase (Stratagene Cloning Systems, La Jolla, CA). The hybridization buffer contained 75% formamide, 10% dextran sulfate, 3 \times SSC, 1 \times Denhardt's, 50 mM sodium phosphate, pH 7.4, and 0.5 ng/ μ l of the probe. After incubation with the probe for 16–18 hr at 55°C, the sections were washed with 2 \times SSC and 1 \times SSC at 55°C, followed by a wash with 0.5 \times SSC for 1 hr at 55°C. The sections then were incubated with nonfat milk, and the sites of PLP mRNA were revealed by incubating with anti-digoxigenin antibody conjugated with alkaline phosphatase (1:250) for 2 hr at RT, and 5-bromo-4-chloro-3-indolyl phosphate (BCIP) with nitroblue tetrazolium (NBT) for 2–3 hr at RT. Two sections from each mouse, separated by

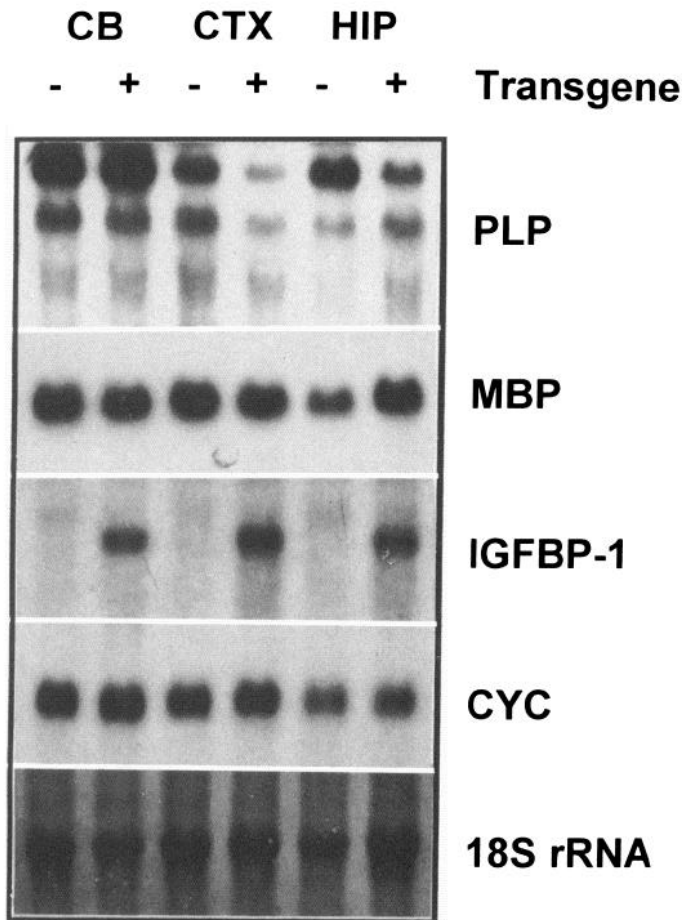


Figure 4. Expression of PLP and MBP genes in cerebral cortex (CTX), hippocampus (HIP) and cerebellum (CB) of 35 d old IGFBP-1 mice. Ten micrograms of total RNA from tissues of IGFBP-1 Tg mice and their littermate controls were applied to each lane. IGFBP-1 Tg mice are indicated as (+) on the top of the figure, and littermate controls as (-). After hybridized with the PLP probe and autoradiography, the filters were stripped and reprobed with MBP, IGFBP-1, and cyclophilin (CYC) probes. The 18S rRNA panel shows methylene blue staining of 18 rRNA band on blot.

at least 50 μm to avoid double counting, were counterstained with methylene green, and photographed. The PLP mRNA-positive oligodendrocytes were counted on the color prints. For each mouse 250–1000 cells (as recognized by nucleus) per area were counted. Liver served as a negative control in which no hybridization signal was observed.

Statistics. Statistic comparisons were made using Student's *t* test.

Results

As demonstrated in previous report, brain growth in IGF-I Tg mice was significantly increased (Mathews et al., 1988; Carson et al., 1993) and that of IGFBP-1 Tg mice decreased (D'Ercole et al., 1994). At 35 d of age, whole brain weight was increased by $34.19 \pm 2.76\%$ (mean \pm SE; $n = 4$; $p < 0.001$) in IGF-I Tg mice and decreased by $12.20 \pm 3.70\%$ ($n = 6$; $p < 0.01$) in IGFBP-1 Tg mice, compared to their normal littermates (Fig. 1). To determine the regional alterations in brain growth, brains from 35 d old IGF-I and IGFBP-1 Tg mice, as well as their nontransgenic littermates, were dissected into distinct regions and wet weights determined (Fig. 1). In IGF-I Tg mice, all brain regions also were increased in weight, with the most affected regions being cerebral cortex, hippocampus, and diencephalon

(increases of $43.18 \pm 7.30\%$, $p < 0.001$; $36.77 \pm 5.57\%$, $p < 0.01$; and $27.55 \pm 6.80\%$, $p < 0.05$, respectively) followed by the brainstem and cerebellum ($24.71 \pm 0.87\%$, $p < 0.001$, and $20.42 \pm 5.70\%$, $p < 0.05$, respectively). As with the IGF-I Tg mice, the cerebral cortex, hippocampus, and diencephalon of IGFBP-1 Tg mice were the most affected brain regions, being decreased by $18.3 \pm 1.51\%$ ($p < 0.001$), $19.89 \pm 1.52\%$ ($p < 0.05$) and $12.28 \pm 1.30\%$ ($p < 0.05$), respectively. The weights of the brainstem and cerebellum in IGFBP-1 mice were more modestly decreased ($7.28 \pm 1.41\%$, $p < 0.05$ and $5.95 \pm 1.57\%$, $p < 0.1$, respectively). There was no difference in brain weight between male and female Tg mice of either line or in their normal littermates, and therefore, the data from both sexes were grouped here and in further analyses.

Morphologically, the size of most brain structures also was increased in IGF-I Tg mice and decreased in IGFBP-1 Tg mice (Fig. 2), but no obvious abnormalities were observed. Compared to their normal littermates, the intensity of myelin staining was markedly increased in IGF-I Tg mice and reduced in the IGFBP-1 Tg mice. The increased myelin staining in IGF-I Tg mice was especially notable in layers III to VI of cerebral cortex, anterior commissure (AC), corpus callosum, diencephalon, and brainstem, while in IGFBP-1 Tg mice, the decrease in myelin staining also was apparent in cerebral cortex, AC, corpus callosum, and diencephalon, but not in brainstem and cerebellum (Fig. 2). High-magnification examination showed that the number of stained fibers was dramatically increased in posterior part of AC (Fig. 2*d*) while they were decreased in IGFBP-1 Tg mice (Fig. 2*f*). Similar results were observed in other brain regions including frontal cerebral cortex and corpus callosum (data not shown).

To determine whether the changes in myelin staining in these Tg mice were due to changes in the number of myelinated axons or the thickness of myelin sheaths, the AC was examined by electron microscopy. Representative electron micrographs of posterior part of AC from 68 d old mice were given in Figure 2*g–i*. The AC was chosen because its myelination was apparently altered under light microscopic examination of these mice and because it is rich in myelinated axons that are in same orientation. Six to nine thousand axons from each anterior and posterior part of AC in each group mice were counted, and the number of myelinated axons in both IGF-I and IGFBP-1 Tg mice was expressed as a percentage of the total number of axons. In non-Tg control mice the percentage of myelinated axons in anterior part of the AC was much higher than posterior part, and the number of myelinated axons in both portions increased with age (Table 1). Similar changes have been observed during development of the AC in rats (Berbel et al., 1994). In both lines of Tg mice, the number of myelinated axons also increased with age in both anterior and posterior portions of the AC. In IGFBP-1 Tg mice, the percentage of myelinated axons in the anterior part of the AC was decreased by 24% and 9% at 35 and 68 d of age, respectively, compared to non-Tg controls. While in IGF-I Tg mice the percentage of myelinated axons was increased, these changes were not significant. In contrast to the anterior part, the number of myelinated axons in the posterior part of the AC in IGF-I Tg mice was increased by 12% at 35 d of age and further increased by 34% at 68 d of age, while the number of myelinated axons in IGFBP-1 mice also was decreased by 42% and 24% at 35 d at 68 d of age, respectively.

The thickness of myelin sheaths was measured in both anterior and posterior parts of the AC from mice at 68 d of age. The

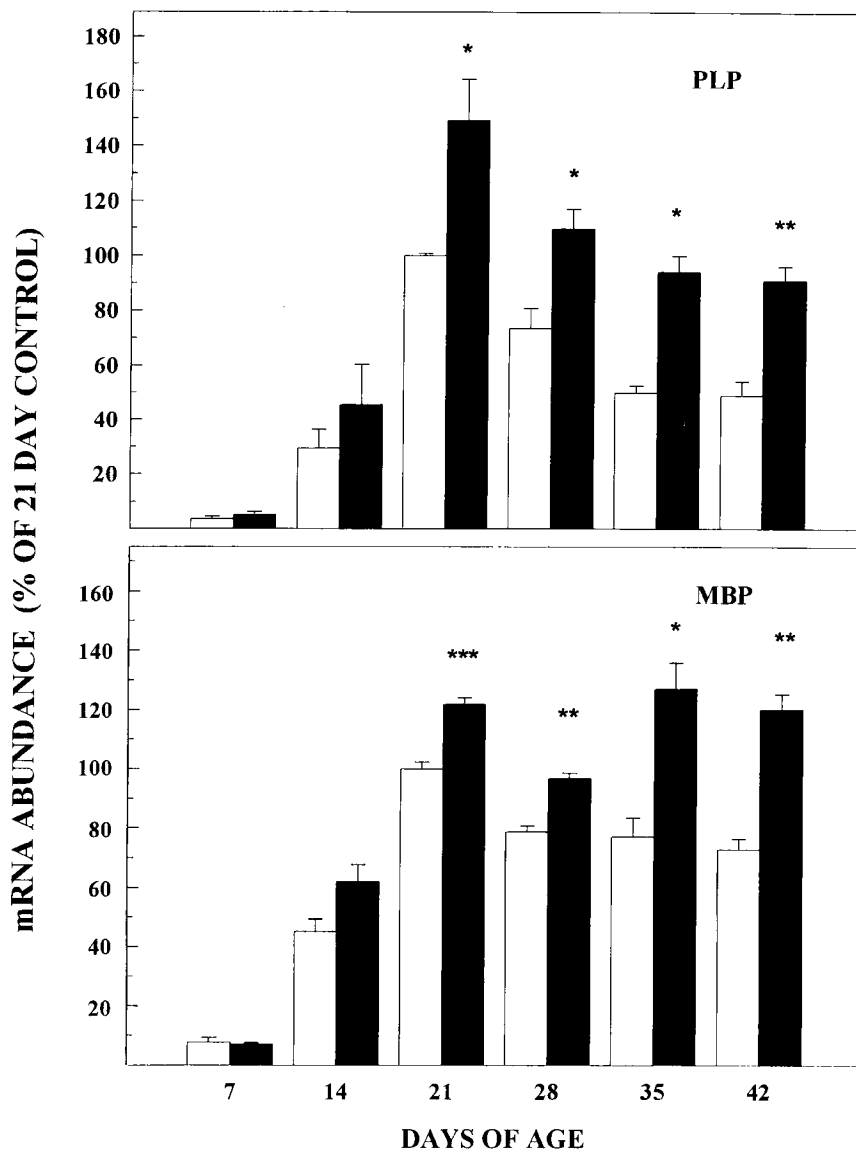


Figure 5. Expression of PLP (*upper panel*) and MBP (*lower panel*) genes in the cerebral cortex of IGF-I Tg mice during postnatal development. PLP and MBP mRNA levels are expressed as percentage of the mRNA levels in normal mice at 21 d of age. Values represent means \pm SE from three to six mice. *, $P < 0.05$; **, $P < 0.01$; ***, $P < 0.001$, compared to normal littermates.

structure of myelin as well as axon appeared normal. Compared to normal control mice (83.04 ± 1.16 nm, mean \pm SE), the thickness of myelin sheaths in anterior part was significantly increased in IGF-I Tg mice (91.76 ± 0.83 , $p < 0.05$), but only modestly decreased in IGFBP-1 Tg mice (77.81 ± 0.64 , $p < 0.15$, n.s.). The thickness of myelin sheaths in posterior portion was generally less than that in anterior part of the AC. Nevertheless, the thickness of myelin sheaths also was increased in IGF-I Tg mice (77.94 ± 0.93 nm, SE, $p < 0.001$) and decreased in IGFBP-1 Tg mice (67.05 ± 0.73 , $p < 0.001$) versus normal control (71.87 ± 0.84).

In general, the thickness of myelin sheaths correlates with the diameter of the axons which they ensheath, that is, the larger axons possess thicker myelin sheaths (Hildebrand et al., 1993). We found that the diameter of myelinated axons was increased in IGF-I Tg mice (592.67 ± 6.21 and 572.44 ± 9.40 nm, mean \pm SE, $p < 0.05$ and $p < 0.001$, in anterior and posterior AC, respectively) versus normal control (574.22 ± 6.85 and 528.62 ± 9.17 nm), and unchanged in IGFBP-1 Tg mice (567.60 ± 6.23 and 529.72 ± 7.48 nm). To eliminate the possible influence of axon diameter on myelin sheath thickness in these Tg mice, the ratio of myelin sheath thickness to axon diameter was cal-

culated and showed an absolute increase in myelin thickness in IGF-I Tg mice (data not shown). To further address this issue, the thickness of myelin sheaths was analyzed in axons of similar diameter (Table 2). Myelin sheath thickness in IGF-I Tg mice was increased in both anterior and posterior AC regardless of the axon diameter, compared to those of their nontransgenic littermates, while the thickness of myelin sheaths was modestly decreased in IGFBP-1 Tg mice.

To evaluate changes in myelin protein gene expression in IGF-I Tg and IGFBP-1 Tg mice, PLP and MBP mRNA abundance was measured. Representative Northern analyses of 35 d old brains are shown in Figures 3 and 4. In IGF-I Tg mice PLP and MBP mRNA levels were significantly increased in cerebral cortex and hippocampus, but minimally or not increased in diencephalon, cerebellum and brainstem (Fig. 3). In IGFBP-1 Tg mice, PLP mRNA levels were significantly reduced in cerebral cortex and hippocampus, but not in cerebellum (Fig. 4).

Next we evaluated the abundance of these mRNAs during development. During cerebral cortex development in normal mice, both PLP and MBP mRNA levels are very low at 7 d of age, but rapidly increase by 14 d of age and reach a peak at 21 d of age, followed by a gradual decline in the next weeks (Figs.

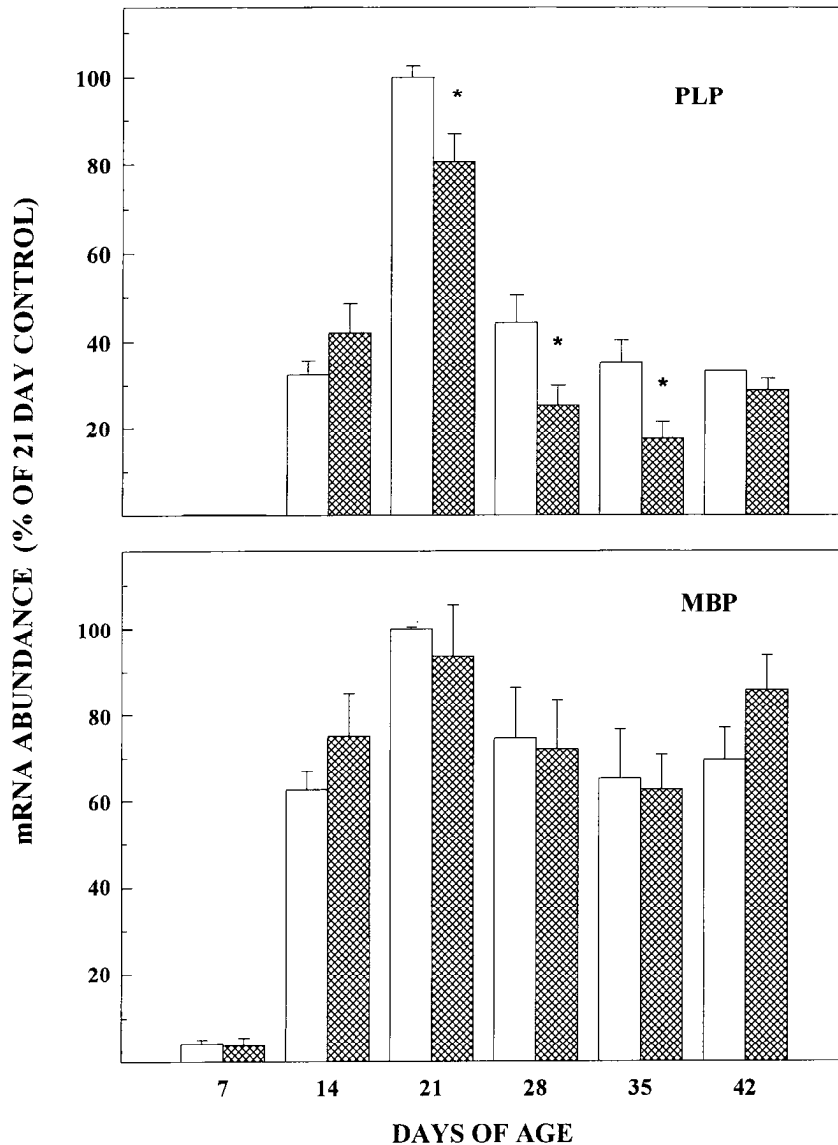


Figure 6. Expression of PLP (upper panel) and MBP (lower panel) in cerebral cortex of IGFBP-1 Tg mice during postnatal development. PLP and MBP mRNA levels are expressed as percentage of the mRNA levels in normal mice at 21 d of age. Values represent means \pm SE from three to six mice. *, $P < 0.05$; compared to normal littermates.

5, 6). In both IGF-I Tg and IGFBP-1 Tg mice, cerebral cortex PLP and MBP mRNA expression exhibited the same developmental pattern as seen in normal mice, with maximal expression occurring at 21 d of age (Figs. 5, 6). Compared to their normal littermates, however, IGF Tg mice expressed an increase of PLP and MBP mRNA abundance at 21 d of age (about 45% and 20% increases, respectively), and the elevated abundance of the mRNAs was maintained, being 80% to 100% increased at both 35 and 42 d of age. On the other hand, the PLP mRNA levels were markedly decreased in IGFBP-1 Tg mice at 21 (~20%), 28 (~40%), and 35 (~50%) d of age, before nearing normal levels at 42 d of life. Although the MBP mRNA levels in IGFBP-1 Tg mice were slightly decreased at 21, 28, and 35 d of age, no significant differences were observed, probably due to the large variations among mice.

To determine if the alterations in cerebral cortex PLP mRNA expression were related to changes in the expression of the transgenes, the abundance of IGF-I and IGFBP-1 transgene mRNAs also was measured. We found that the changes in myelin protein mRNA levels correlated with both the regional (Figs. 3, 4, 7) and temporal (Fig. 8) expression of both transgene mRNAs. In

35 d old IGF-I Tg mice, the IGF-I transgene mRNA was most highly expressed in cerebral cortex and hippocampus, where PLP and MBP mRNAs levels exhibited the most markedly elevations (Figs. 3, 7). The levels of IGF-I transgene mRNA were only 10, 3, and 2% of cerebral cortex levels in diencephalon, brainstem and cerebellum, respectively (Figs. 3, 7). During development (Fig. 8, upper panel), cerebral cortex IGF-I transgene mRNA levels were relatively low at 7 d of age, rapidly increased from 14 to 28 d (1.11 ± 0.13 , 2.23 ± 0.29 , and 2.91 ± 0.54 -fold increases at 14, 21, and 28 d of age, respectively, compared to the abundance at 7 d; mean \pm SE; $n = 4$ or 5), after which the transgene's expression remained stable. The increase in IGF-I transgene mRNA levels paralleled with the changes in PLP mRNA levels.

Like IGF-I transgene mRNA, IGFBP-1 transgene mRNA in 35 d old brains was most abundant in cerebral cortex, and was 83 and 75% of cerebral cortex levels in hippocampus and cerebellum, respectively (Figs. 4, 7). Cerebral cortex IGFBP-1 mRNA was very low before 9 d of age, and rapidly increased by 14 and 21 d (2.19 ± 0.35 and 4.17 ± 0.56 -fold increases, respectively, compared to its abundance at 9 d of age; mean \pm

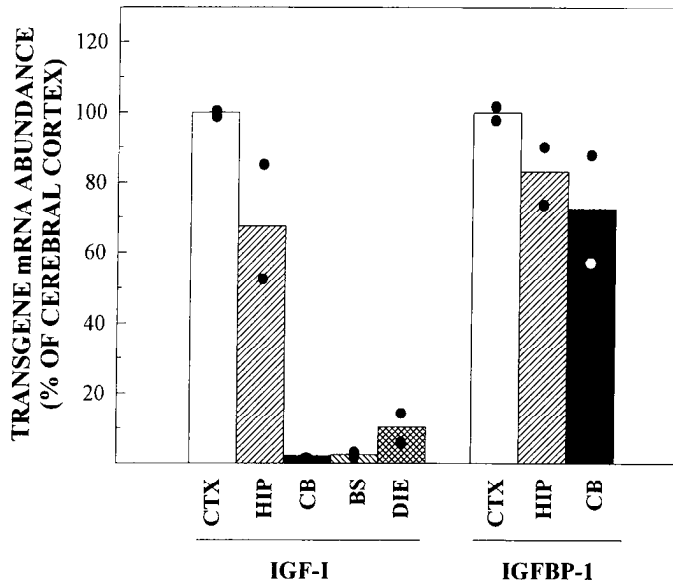


Figure 7. Regional brain IGF-I and IGFBP-1 transgene expression. Brains from 35 d old IGF-I Tg mice and IGFBP-1 Tg mice were dissected. The abundance of transgene mRNAs is expressed as percentage of cerebral cortex levels. Bars are the means of two mice, and dots are actual values. CTX, Cerebral cortex; HIP, hippocampus; CB, cerebellum; BS, brainstem; DIE, diencephalon.

SE; $n = 4$) (Fig. 8, lower panel). With the increase of IGFBP-1 transgene mRNA, PLP mRNA levels gradually decreased reaching their lowest levels at 28–35 d. The abundance of both transgene mRNAs in hippocampus, cerebellum exhibited a same developing pattern (data not shown). This pattern of IGF-I and IGFBP-1 transgene expression is consistent with that of endogenous MT-1 mRNA in the mouse brain (Shiraidhi et al., 1991).

If the brain growth retardation and decreased PLP expression in the IGFBP-1 Tg mice is the result of inhibition of endogenous IGF-I actions, then IGFBP-1 expression would be expected to blunt or ablate the brain overgrowth in IGF-I Tg mice. To test this possibility we bred male IGF-I Tg mice with female IGFBP-1 Tg mice and assessed brain weights and the expression of myelin-specific protein genes at 35 d of age (Table 3). The brains of the mice carrying both IGF-I and IGFBP-1 transgenes were significantly smaller than those of IGF-I Tg mice, but were larger than those of their normal littermate controls and IGFBP-1 Tg mice. All brain regional weights bore the same relationships, except for the cerebellum which did not appear to be affected by IGFBP-1 expression. In IGF-I Tg mice cerebral cortex PLP and MBP mRNA abundance was increased about three- and twofold, respectively, and was significantly blunted by IGFBP-1 transgene expression (Table 4).

To determine whether the changes in the expression of PLP and MBP mRNAs in these Tg mice were due to a change in the number of functional oligodendrocytes, we performed *in situ* hybridization with a probe to PLP mRNA, and the PLP mRNA-positive oligodendrocytes in corpus callosum and frontal cerebral cortex (layers 2–6) were counted. As previously reported (Verty and Campagnoni, 1988; Jordan et al., 1989; Shiota et al., 1989), we found that PLP mRNA is predominantly localized to the cell body of oligodendrocytes. The total number of labeled oligodendrocytes was significantly increased in IGF-I Tg mice and decreased in IGFBP-1 Tg mice (Fig. 9, Table 5). The per-

centage of PLP mRNA-labeled oligodendrocytes in IGF-I Tg mice was increased by $18.14 \pm 1.64\%$ ($n = 3$; $p < 0.001$) and $36.52 \pm 8.44\%$ ($p < 0.01$) in corpus callosum and cortex, respectively. The intensity of PLP mRNA labeling also appeared increased in these Tg mice. The percentage of PLP mRNA-labeled oligodendrocytes in IGFBP-1 mice was decreased by $4.99 \pm 1.03\%$ ($n = 3$; $p < 0.05$) and $18.36 \pm 6.39\%$ ($p < 0.2$, n.s.) in corpus callosum and cortex, respectively.

Discussion

Our data strongly support a role for IGF-I in promoting oligodendrocyte development and stimulating oligodendrocyte function. We demonstrate here that overexpression of IGF-I in brain greatly increases the number of myelinated axons and the thickness of myelin sheaths, associated with increases in the number of oligodendrocytes and the expression of myelin protein genes. These results are consistent with previous report of a marked increase in total brain myelin content in IGF-I Tg mice (Carson et al., 1993). In contrast to IGF-I Tg mice, the retardation of brain growth in the Tg mice that exhibit ectopic brain expression of IGFBP-1, an inhibitor of IGF action when it is present in molar excess (Hakala-Ala-Pietila et al., 1993; Shambaugh et al., 1993; Verhaeghe et al., 1993; Jones and Clemmons, 1995), is accompanied by a decrease in the percentage of PLP mRNA-expressing oligodendrocytes and in the abundance of the myelin-specific protein mRNA, and a dramatic decrease in the number of myelinated axons. We also show that increased myelin specific gene expression in IGF-I Tg mice, as well as the brain overgrowth, is blunted by coexpression of the IGFBP-1 transgene, strongly indicating that expression of the IGFBP-1 in brain inhibits IGF-I actions regardless of whether IGF-I is endogenously derived or is synthesized by the transgene.

During development the increase in the expression of myelin protein gene in cerebral cortex of IGF-I Tg mice correlates regionally and temporally with the increase of IGF-I transgene mRNA levels. The regional brain growth also is closely associated with regional levels of IGF-I transgene mRNA. Furthermore, in the IGFBP-1 Tg mice the abundance of myelin protein mRNAs declines in temporal association with the rise in the expression of the IGFBP-1 transgene. These data indicate that the changes in myelin protein gene expression, resulting in changes in myelination and brain growth, are dependent upon local transgene expression. The timing of the rise in the expression of both transgenes is the result of their MT-1 promoter, because the expression of both transgenes follows the same developmental pattern as does MT-1 mRNA in mouse brain (Shiraidhi et al., 1991). The transient decrease in myelin protein gene expression in IGFBP-1 Tg mice is consistent with our findings that the decreased percentage of myelinated axons in the AC of IGFBP-1 Tg mice becomes less with age (decreases of 24% vs 9% in anterior part, and 42% vs 24% in posterior part at 35 and 68 d of age, respectively). We speculate that the transiency of IGFBP-1's effects on myelination are related to the decrease in endogenous IGF-I expression with advancing age (Rotwein et al., 1988; Bartlett et al., 1991). In other words, as IGF-I expression in brain declines and in turn its effects on myelination diminish, the influence of the IGFBP-1 transgene is ablated. This also implies that factors other than IGF-I can subserve its role in stimulating myelination.

In contrast to the marked decreases in myelinated axon number in IGFBP-1 Tg mice, the increases in myelinated axons in anterior AC of IGF-I Tg mice were minimal. High expression

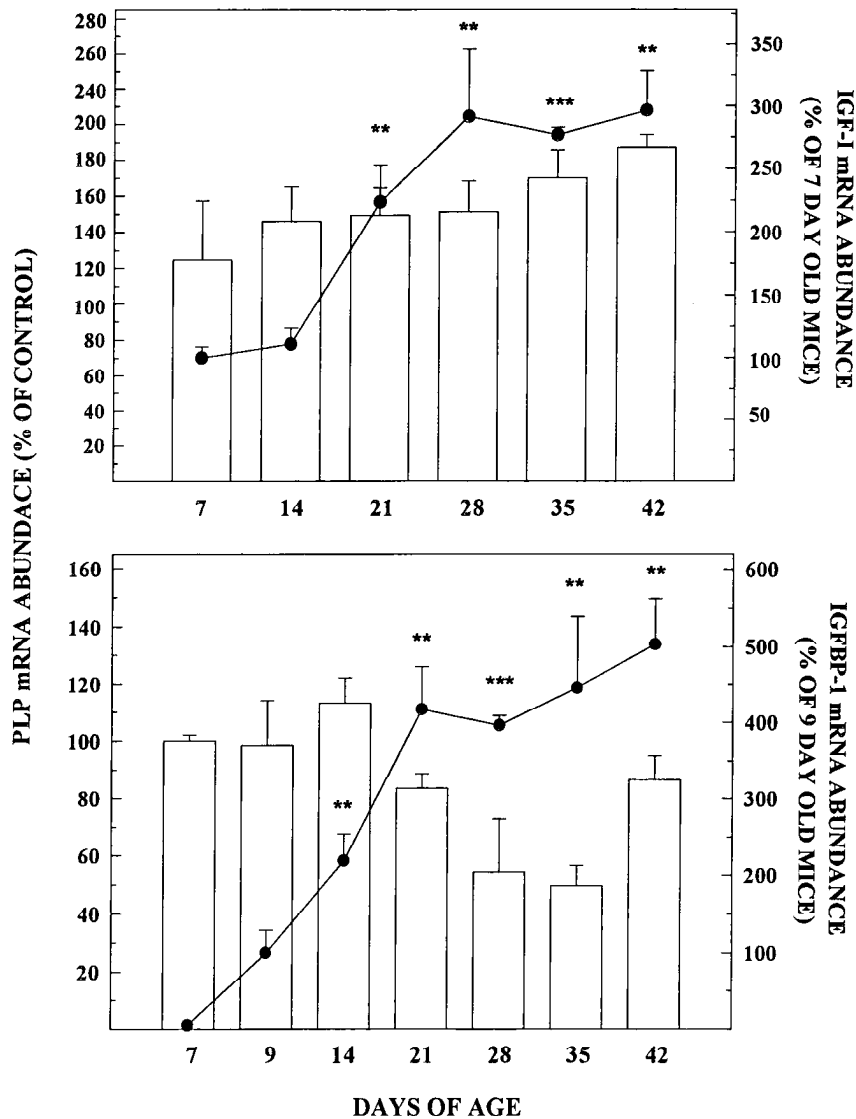


Figure 8. Cerebral cortex PLP gene expression in relation to the expression of the IGF-I (upper panel) and the IGFBP-1 transgene (lower panel) during development. PLP mRNA abundance (open bars) is presented as percentage of their normal littermate controls. IGF-I and IGFBP-1 transgene mRNA abundance (solid circles) is presented as percentage of the mRNA abundance of 7 and 9 d old mice, respectively. Values represent means \pm SE of three to six mice. *, $P < 0.05$; **, $P < 0.01$; ***, $P < 0.001$; compared to 7 d old IGF-I Tg mice or 9 d old IGFBP-1 Tg mice, respectively.

of endogenous IGF-I in olfactory bulb (Rotwein et al., 1988; Bach et al., 1991), the origin of the axons in anterior portion of AC, may have nearly maximized IGF-I effects, and thus blunted the effect of the transgene. The dramatic effect of IGFBP-1 on myelinated axon number in the anterior AC is consistent with this hypothesis because IGFBP-1 blocks the actions of endogenous IGF-I. The modest decreases in myelin thickness in IGFBP-1 Tg mice may be caused by the normally large variation in brain myelinated axon characteristics, that is, axon diameter

and myelin sheath thickness. For examples, axon diameters in normal mice range from 200 to 1200 nm (our data; Hildebrand et al., 1993).

Our findings that the myelin protein mRNA abundance in cerebellum is not altered in IGFBP-1 overexpressing mice, and that expression of the IGFBP-1 transgene has little influence on cerebellar size, is consistent with the developmental time of the expression of these MT-1-driven transgenes. Myelination in cerebellum occurs earlier than other forebrain regions (Jacobson,

Table 3. Brain weights in IGF-I Tg mice, IGFBP-1 Tg mice, Tg mice carrying both transgenes, and their normal littermates

Genotype (IGF-I/IGFBP-1)	Body and brain weights (gm. means \pm SE)		
	Body	Whole brain	Cerebellum
/-	20.47 \pm 1.65 (5)	0.46 \pm 0.01 (5)	0.054 \pm 0.01 (5)
+/-	19.21 \pm 1.42 (5)	0.61 \pm 0.01 (5)*	0.070 \pm 0.04 (5)*
-/+	19.29 \pm 1.60 (3)	0.40 \pm 0.01 (3)*	0.053 \pm 0.01 (3)
+/+	19.00 \pm 3.20 (3)	0.53 \pm 0.01 (3)*!	0.068 \pm 0.02 (3)*

At 35 d of age, two litters of mice were sacrificed, and brains dissected and weighed. Values represent means \pm SE. The number of mice is given in parentheses. *, $p < 0.01$, compared to normal littermates. !, $p < 0.01$, compared to IGF-I/- mice.

Table 4. Expression of cerebral cortex PLP and MBP genes in IGF-I Tg mice, IGFBP-1 Tg mice, and Tg mice carrying both IGF-I and IGFBP-1 transgenes

	Expression of myelin protein genes (% of control, means \pm SE)	
	PLP mRNA	MBP mRNA
Littermate control	100.00 \pm 2.20	100.00 \pm 5.07
IGF-I Tg	343.36 \pm 63.84*	170.89 \pm 14.67*
IGFBP-1 Tg	61.01 \pm 11.98*	98.92 \pm 18.71
IGF-I/IGFBP-1 Tg	138.50 \pm 9.39+	125.66 \pm 21.62

Values represent means \pm SE of three to six mice. +, $p < 0.2$; *, $p < 0.05$; **, $p < 0.01$, compared to normal littermates.

1963; Caley and Maxwell, 1968; Okado, 1982; Foran and Peterson, 1992) and prior to the time of peak expression of IGFBP-1 transgene. Although the transgene is expressed well in cerebellum (slightly lower than cerebral cortex), therefore, its effects are not dramatic because of its relatively late expression in cerebellum during development.

We used *in situ* hybridization with a probe for PLP mRNA to identify oligodendrocytes actively synthesizing this myelin specific protein. IGF-I Tg mice had an increase in the number of oligodendrocytes in the cerebral cortex and corpus callosum, as judged by their percentage representation, while in IGFBP-1 Tg mice oligodendrocyte number was decreased in corpus callosum (the decrease observed in cerebral cortex was not significant). These results suggest that the total number of oligoden-

Table 5. Relative oligodendrocyte number in corpus callosum and cerebral cortex of IGF-I and IGFBP-1 Tg mice

	Number of oligodendrocyte (% of total cells, means \pm SE)	
	Corpus callosum	Cerebral cortex
Littermate controls	55.15 \pm 0.67	12.34 \pm 1.12
IGF-I Tg	65.19 \pm 0.89***	16.84 \pm 1.04**
IGFBP-1 Tg	52.40 \pm 0.57*	10.07 \pm 0.79+

Brains from 35 d old mice of IGF-I Tg, IGFBP-1 Tg, and normal littermate mice were frozen-sectioned sagittally. Oligodendrocytes were identified by PLP mRNA *in situ* hybridization. A PLP mRNA-positive cell was defined as a methylene green stained nucleus surrounded by brown-purple *in situ* hybridization staining. The number of PLP mRNA-positive cells is presented as percentage of total cells. Values are means \pm SE of three mice. +, $p < 0.2$; *, $p < 0.05$; **, $p < 0.01$; ***, $p < 0.001$, compared to normal littermates.

drocytes, as well as their relative number compared to other cell types, is increased in IGF-I Tg and decreased in IGFBP-1 Tg mice. These data also suggest that IGF-I plays a role in controlling oligodendrocyte development, proliferation and/or survival. *In vitro* studies strongly support this conclusion, because IGF-I has been shown to substantially increase oligodendrocyte number both by increasing the proliferation and differentiation of progenitor cells (McMorris et al., 1988) and by increasing survival of oligodendrocytes (Barres et al., 1992).

Carson et al. (1993), using immunostaining with an antibody to carbonic anhydrase II (CA-II) to identify oligodendrocytes in IGF-I Tg mice, however, did not find an increase in the per-

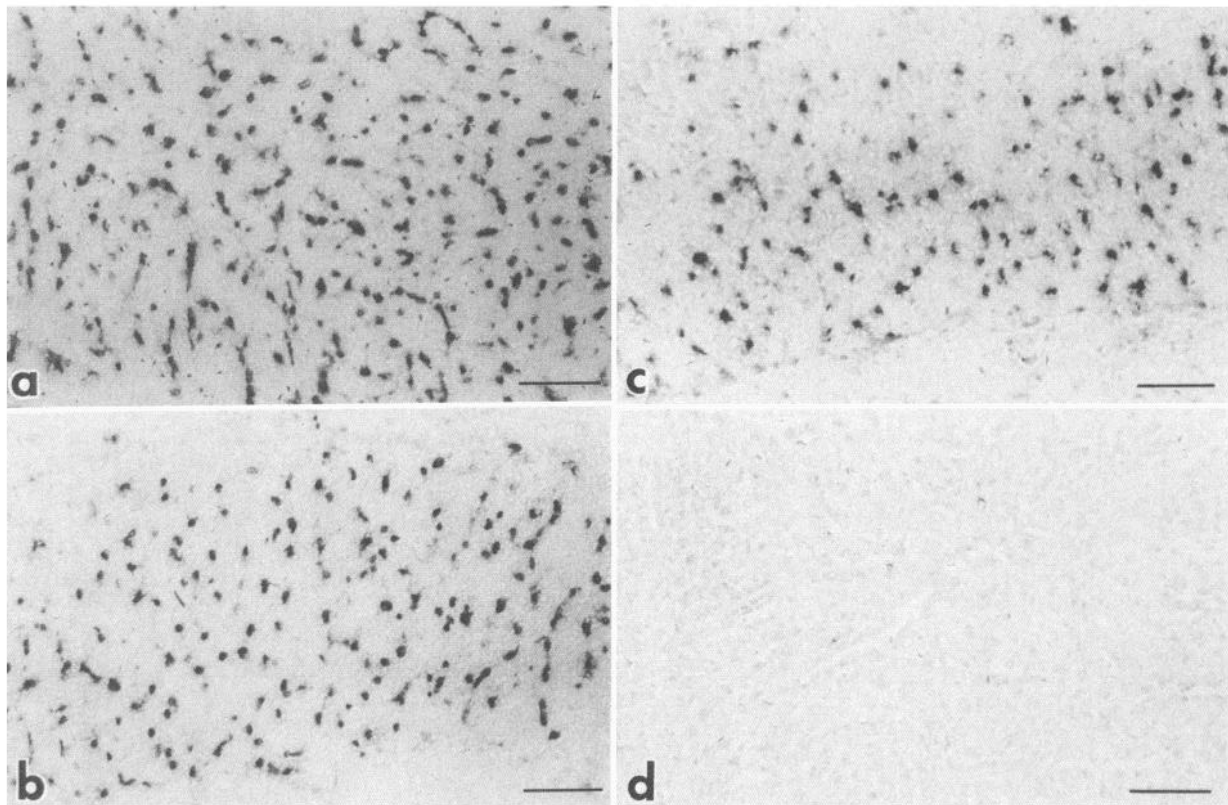


Figure 9. PLP mRNA-labeled oligodendrocytes in corpus callosum of IGF-I and IGFBP-1 Tg mice. Brains from 35 d old IGF-I Tg (*a*) and IGFBP-1 Tg (*c*) mice, as well as normal littermate mice (*b*) were frozen-sectioned sagittally, and hybridized with digoxigenin-labeled PLP cRNA probe without counterstaining. Liver (*d*) served as negative control. Scale bars, 50 μ m.

centage of immunostained oligodendrocytes in IGF-I Tg mice. In our studies a different IGF-I Tg mice line was utilized. In addition, while the percentage of oligodendrocytes determined by PLP mRNA-labeling in corpus callosum agrees with the percentage reported by CA-II immunostaining, we obtained a higher percentage of oligodendrocytes in the cerebral cortex of normal mice (10% compared to >5%). The sensitivity of *in situ* hybridization and high abundance of PLP mRNA in oligodendrocytes may explain this discrepancy. Recent reports indicate that CA-II may not be entirely specific for oligodendrocytes (Cammer and Zhang, 1991, 1992; Jeffery et al., 1991) and the CA-II antibody does not recognize all oligodendrocytes (Berry, personal communication). Although we believe that our results reflect an increase in oligodendrocyte number in IGF-I Tg mouse brains, they undoubtedly demonstrate an increase in the number of oligodendrocytes that are actively expressing PLP.

The changes in the percentage of PLP mRNA-positive cells, however, do not completely account for the changes in myelin-specific protein mRNAs in these Tg mice. In IGFBP-1 Tg mice, the percentage of oligodendrocytes was not markedly decreased in cerebral cortex (~18%) or in corpus callosum (~5%), compared to littermate controls, while PLP mRNA levels were decreased by 40–50%. Similarly, the increase in the percentage of oligodendrocytes (~37% and ~18% in cerebral cortex and corpus callosum, respectively) does not reflect the two- to threefold increases in PLP and MBP mRNA levels found in IGF-I Tg mice. The alterations of myelin protein mRNA abundance, therefore, must be due to changes in the gene expression of individual oligodendrocytes, in addition to changes in the number of oligodendrocytes, and thus indicate a stimulation of oligodendrocyte functions by IGF-I.

Data of others point to direct IGF-I actions on oligodendrocytes, because (1) oligodendrocytes express type I IGF receptors, (2) IGF-I promotes oligodendrocytes proliferation and/or survival *in vitro* (McMorris et al., 1986; Mozell and McMorris, 1991; Barres et al., 1992), (3) fewer of oligodendrocyte progenitors mature in cultured embryonic forebrain from type I IGF receptor knock-out mutant mice (Liu et al., 1993), and (4) mice with disrupted expression of the IGF-I gene exhibit a reduction in oligodendrocyte development (Beck et al., 1995). Because neurons interact with oligodendrocytes and because IGF-I has been shown to stimulate neuron proliferation and development *in vitro* (Torres-Aleman et al., 1990, 1992; Bartlett et al., 1991; Garcia-Segura et al., 1991; Pahlman et al., 1991), we can not exclude the possibility that IGF-I's effects on oligodendrocyte number and myelination are indirect and mediated by neurons. Our data, however, clearly demonstrate that the myelin thickness is increased in IGF-I Tg mice in a fashion that is independent of axon diameter. If IGF-I were to increase oligodendrocyte number by increasing the number of neurons and axons, one would not expect increases in the percentage of oligodendrocytes, in the percentage of myelinated axons or increases in absolute myelin thickness (all results of our study). Our data, therefore, support direct effects of IGF-I on oligodendrocytes and myelination, but do not exclude IGF-I effects on neuron proliferation/survival and/or maturation. In summary, we hypothesize that IGF-I stimulates oligodendrocytes in two phases: (1) stimulation of oligodendrocyte proliferation, differentiation and/or survival during early development (prior to postnatal weeks of life) and (2) stimulation of myelin gene expression and myelin production (after 2 weeks of life).

References

- Bach MA, Shen-Orr Z, Lower WL Jr, Roberts CT Jr, LeRoith D (1991) Insulin-like growth factor I mRNA levels are developmentally regulated in specific regions of the rat brain. *Mol Brain Res* 10:43–48.
- Baron-Van Evercooren A, Olichon-Berthe C, Kowalski A, Visciano G, Van Obberghen E (1991) Expression of IGF-I and insulin receptor genes in the rat central nervous system: a developmental, regional, and cellular analysis. *J Neurosci Res* 28:244–253.
- Barres BA, Hart IK, Coles HSR, Burrne JF, Voyvodic JT, Richardson WD, Raff MC (1992) Cell death and control of cell survival in the oligodendrocyte lineage. *Cell* 70:31–46.
- Barres BA, Raff MC (1993) Proliferation of oligodendrocyte precursor cells depends on electrical activity in axons. *Nature* 21:258–260.
- Bartlett WP, Li X-S, Williams M, Benkovic S (1991) Localization of insulin-like growth factor-I mRNA in murine central nervous system during postnatal development. *Dev Biol* 147:239–250.
- Beck KD, Powell-Braxton L, Widmer H-R, Valverde J, Hefti F (1995) *Igf1* gene disruption results in reduced brain size, CNS hypomyelination, and loss of hippocampal granule and striatal parvalbumin-containing neurons. *Neuron* 14:717–730.
- Behringer RR, Lewin TM, Quaife CJ, Palmiter RD, Brinster RL, D'Ercole AJ (1990) Expression of insulin-like growth factor I stimulation normal somatic growth in growth hormone-deficient transgenic mice. *Endocrinology* 127:1033–1040.
- Berbel P, Guadano-Ferraz A, Angulo A, Cerezo JR (1994) Role of thyroid hormone in the maturation of interhemispheric connections in rats. *Behav Brain Res* 64:9–14.
- Brewer MT, Stetler GL, Squires CH, Thompson RC, Busby WH, Clemmons DR (1988) Cloning, characterization, and expression of a human insulin-like growth factor binding protein. *Biochem Biophys Res Commun* 152:1289–1297.
- Caley DW, Maxwell DS (1968) An electron microscopic study of the neuroglia during postnatal development of the rat cerebrum. *J Comp Neurol* 133:45–70.
- Cammer W, Zhang H (1991) Comparison of immunocytochemical staining of astrocytes, oligodendrocytes, and myelinated fibers in the brains of carbonic anhydrase II-deficient mice and normal littermates. *J Neuroimmunol* 34:81–86.
- Cammer W, Zhang H (1992) Carbonic anhydrase in distinct precursors of astrocytes and oligodendrocytes in the forebrains of neonatal and young rats. *Dev Brain Res* 67:257–263.
- Campagnoni AT (1988) Molecular biology of myelin proteins from the central nervous system. *J Neurochem* 51:1–14.
- Carson MJ, Behringer RR, Brinster RL, McMorris FA (1993) Insulin-like growth factor I increases brain growth and central nervous system myelination in transgenic mice. *Neuron* 10:729–740.
- Chen SJ, DeVries GH (1989) Mitogenic effect of axolemma-enriched fraction on cultured oligodendrocytes. *J Neurochem* 52:325–327.
- Chomczynski P, Sacchi N (1987) Single-step method of RNA isolation by acidic guanidinium thiocyanate-phenol-chloroform extraction. *Anal Biochem* 162:156–159.
- Dai Z, Xing Y, Boney C, Clemmons DR, D'Ercole AJ (1994) Human insulin-like growth factor-binding protein-1 (IGFBP-1) in transgenic mice: characterization and insights into the regulation of IGFBP-1 expression. *Endocrinology* 135:1316–1327.
- Danielson PE, Forss-Petter S, Brow MA, Calavetta L, Douglass J, Milner RJ, Sutcliffe JG (1988) p1B15: a cDNA clone of the rat mRNA encoding cyclophilin. *DNA* 7:261–267.
- D'Ercole AJ, Dai Z, Xing Y, Boney C, Wikie MB, Lauder JM, Han VKM, Clemmons DR (1994) Brain growth retardation due to the expression of human insulin like growth factor binding protein-1 (IGFBP-1) in transgenic mice: an *in vivo* model for the analysis of IGF function in the brain. *Brain Res Dev Brain Res* 82:312–222.
- Foran OR, Peterson AC (1992) Myelin acquisition in the central nervous system of the mouse revealed by an MBP-Lac Z transgene. *J Neurosci* 12:4890–4897.
- Garcia-Segura LM, Perez L, Pons S, Rejas MT, Torres-Aleman I (1991) Localization of insulin-like growth factor I (IGF-I)-like immunoreactivity in the developing and adult rat brain. *Brain Res* 560:167–174.
- Hakala-Ala-Pietila TH, Koistinen RA, Salonen RK, Seppala MT (1993) Elevated second-trimester amniotic fluid concentration of insulin-like growth factor binding protein-1 in fetal growth retardation. *Am J Obstet Gynecol* 169:35–39.
- Hildebrand C, Remahl S, Persson H, Bjartmar C (1993) Myelinated nerve fibres in the CNS. *Prog Neurol* 40:319–384.

- Hudson LD, Berndt JA, Puckett C, Kozak CA, Lazzarini RA (1987) Aberrant splicing of proteolipid protein mRNA in the dysmyelinating jimpy mutant mouse. *Proc Natl Acad Sci USA* 84:1454–1458.
- Hunter SF, Bottenstein (1991) O-2A glial progenitors from mature brain respond to CNS neuronal cell line-derived growth factors. *J Neurosci Res* 28:574–582.
- Jacobsen S (1963) Sequence of myelination in the brain of the albino rat. A. Cerebral cortex, thalamus and related structures. *J Comp Neurol* 121:5–29.
- Jakubowski M, Blum M, Roberts JL (1991) Postnatal development of gonadotropin-releasing hormone and cyclophilin gene expression in female and male rat brain. *Endocrinology* 128:2702–2708.
- Jansen M, Schaik F, Ricker A, Bullock B, Woods D, Gabbay K, Nussbaum A, Sussenbach J, Van den Brande J (1983) Sequence of cDNA encoding human insulin-like growth factor I precursor. *Nature* 306:609–611.
- Jeffery M, Wells GAH, Bridges AW (1991) Carbonic anhydrase II expression in fibrous astrocytes of the sheep. *J Comp Pathol* 104:337–343.
- Jones JI, Clemmons (1995) Insulin-like growth factors and their binding proteins: biological actions. *Endocrine Rev* 16:3–34.
- Jordan C, Friedrich V Jr, Dubois-Dalq M (1989) *In situ* hybridization analysis of myelin gene transcripts in developing mouse spinal cord. *J Neurosci* 9:248–257.
- Konat G, Laszkiewicz I, Bednarczuk T, Kanoh M, Wiggins RC (1991) Generation of radioactive and nonradioactive ssDNA hybridization probes by polymerase chain reaction. *Technique* 3:64–68.
- Lee PDK, Conover CA, Powell DR (1993) Regulation and function of insulin-like growth factor-binding protein-1. *Proc Soc Exp Biol Med* 204:4–29.
- Liu J-P, Baker J, Perkins AS, Robertson EJ, Efstratiadis A (1993) Mice carrying null mutations of the genes encoding insulin-like growth factor I (*Igf-1*) and type I IGF receptor (*Igflr*). *Cell* 75:59–72.
- Masters BA, Werner H, Roberts CT Jr, LeRoith D, Raizada MK (1991) Insulin-like growth factor I (IGF-I) receptors and IGF-I action in oligodendrocytes from rat brains. *Regul Pept* 33:117–131.
- Mathews LS, Hammer RE, Behringer RR, D'Ercole AJ, Bell GI, Brinster RL, Palmiter RD (1988) Growth enhancement of transgenic mice expressing human insulin-like growth factor I. *Endocrinology* 123:2827–2833.
- McMorris FA, Dubois-Dalq M (1988) Insulin-like growth factor I promotes cell proliferation and oligodendroglial commitment in rat glial progenitor cells developing *in vitro*. *J Neurosci Res* 21:199–209.
- McMorris FA, Smith TM, DeSalvo S, Furianetto RW (1986) Insulin-like growth factor I/somatostatin C: a potent inducer of oligodendrocyte development. *Proc Natl Acad Sci USA* 83:822–826.
- Mozell RL, McMorris FA (1991) Insulin-like growth factor I stimulates oligodendrocyte development and myelination in rat brain aggregate cultures. *J Neurosci Res* 30:382–390.
- Newman S, Kitamura K, Campagnoni AT (1987) Identification of a cDNA coding for a fifth form of myelin basic protein in mouse. *Proc Natl Acad Sci USA* 84:886–890.
- Okado N (1982) Early myelin formation and glial cell development in the human spinal cord. *Anat Rec* 202:483–490.
- Pahlman S, Meyerson G, Lindgren E, Scjalling M, Johansson I (1991) Insulin-like growth factor I shifts from promoting cell division to potentiating maturation during neuronal differentiation. *Proc Natl Acad Sci USA* 88:9994–9998.
- Raff MC (1989) Glial cell diversification in the rat optic nerve. *Science* 243:1450–1455.
- Rowtein P, Burgess SK, Milbrandt JD, Krause JE (1988) Differential expression of insulin-like growth factor genes in rat central nervous system. *Proc Natl Acad Sci USA* 85:265–269.
- Schmued LC (1990) A rapid, sensitive histochemical stain for myelin in frozen brain sections. *J Histochem Cytochem* 38:717–720.
- Shambaugh GE III, Radosevich JA, Glick RP, Gu DS, Metzger BE, Unterman TG (1993) Insulin-like growth factors and binding proteins in fetal rat: alterations during maternal starvation and effects in fetal brain cell culture. *Neurochem Res* 18:695–703.
- Shiota C, Miura M, Mikkoshiba K (1989) Developmental profile and differential localization of mRNAs of myelin proteins (MBP and PLP) in oligodendrocytes in the brain and in culture. *Dev Brain Res* 45:83–94.
- Shiraishi N, Taguchi T, Kinebuchi H (1991) Metallothionein messenger RNA levels in the macular mutant mouse: an animal model of Menkes' kinky-hair disease. *Biol Neonat* 60:52–61.
- Sorg BA, Smith MN, Campagnoni AT (1987) Developmental expression of the myelin proteolipid protein and basic protein mRNAs in normal and dysmyelinating mutant mice. *J Neurochem* 49:1146–1154.
- Stenvers KL, Zimmermann EM, Gallagher M, Lund PK (1994) Expression of insulin-like growth factor binding protein-4 and -5 mRNAs in adult rat forebrain. *J Comp Neurol* 399:91–105.
- Torres-Aleman I, Naftolin F, Robbins RJ (1990) Trophic effects of insulin-like growth factor-I on fetal rat hypothalamic cells in culture. *Neuroscience* 35:601–608.
- Torres-Aleman I, Pons S, Santos-Benito FF (1992) Survival of Purkinje cell in cerebellar cultures is increased by insulin-like growth factor I. *Eur J Neurosci* 4:864–869.
- Verhaeghe J, Van Bree R, Van Herck E, Laureys J, Bouillon R, Van Assche FA (1993) C-peptide, insulin-like growth factors I and II, and insulin-like growth factor binding protein-1 in umbilical cord serum: correlations with birth weight. *Am J Obstet Gynecol* 169:89–97.
- Verity AN, Campagnoni AT (1988) Regional expression of myelin protein genes in the developing mouse brain: *in situ* hybridization studies. *J Neurosci Res* 21:238–248.
- Ye P, Kanoh M, Zhu W, Laszkiewicz I, Royland JE, Wiggins RC, Konat G (1992) Cyclic AMP-induced upregulation of proteolipid protein and myelin associated glycoprotein gene expression in C6 cells. *J Neurosci Res* 31:578–583.
- Zimmermann EM, Sartor RB, McCall RD, Pardo M, Bender D, Lund PK (1993) Insulin-like growth factor I and interleukin 1 β messenger RNA in a rat model of granulomatous enterocolitis and hepatitis. *Gastroenterology* 105:399–409.